INDIAN JOURNAL OF SCIENCE AND TECHNOLOGY

RESEARCH ARTICLE

Image Segmentation Based on G.O.A for Finding Deformities in Medical and Aura Images

Manjula Poojary[1]*, **Yarramalle Srinivas**[2]

1 Research Scholar, Department of CSE, GITAM Deemed to be University, Visakhapatnam, Andhra Pradesh, India
2 Professor, Department of CSE, GITAM Deemed to be University, Visakhapatnam, Andhra Pradesh, India

OPEN ACCESS

Received: 14-04-2024
Accepted: 06-05-2024
Published: 18-05-2024

Citation: Poojary M, Srinivas Y (2024) Image Segmentation Based on G.O.A for Finding Deformities in Medical and Aura Images. Indian Journal of Science and Technology 17(20): 2117-2127. https://doi.org/10.17485/IJST/v17i20.629

* **Corresponding author**.

mpoojary@gitam.edu

Funding: None

Competing Interests: None

Published By Indian Society for Education and Environment (iSee)

ISSN
Print: 0974-6846
Electronic: 0974-5645

Abstract

Objectives: The research aims to develop the segmentation model to identify the deformity in the medical images as accurately as possible and plan for better medical treatment. The study is extended to identify the disease before its appearance in the human body through human aura images to support aura imaging in medical diagnosis. **Methods:** The study used a brain image from the UCI data set and Aura images from the Biowell data set to identify the disease. The segmentation model Bivariate Gaussian Mixture Model (B.G.M.M) was developed. Model parameters are derived using the Expectation Maximization (E.M) Algorithm. The Grasshopper optimization Algorithm (G.O.A) extracts optimal features from the images. The chosen feature is fed as input to the classification model B.G.M.M. Segmentation accuracy is measured using the quality metrics**. Findings:** The developed approach shows 97% accuracy in identifying the damaged tissues in MRI images and high-intensity energy zones in the aura images, indicating the potential for deformities. **Novelty:** This study significantly contributes to the field by offering novel solutions for precise and comprehensive image analysis in medical and aura imaging contexts.

Keywords: G.O.A; segmentation; G.M.M; E.M; quality metrics; deformity identification; Hue and saturation

1 Introduction

Many methods have been coined in the literature to identify the disease through medical images. Our previous work concentrated on identifying the abnormalities in medical and aura pictures, where we developed the truncated Gaussian mixture model (T.G.M.M) and considered the finite region of the image for deformity identification. A drawback of employing a T.G.M.M is that the truncation threshold may need to be carefully adjusted. Information loss could occur from an inadequate representation of the data distribution caused by a truncation threshold set too low. On the other hand, if the threshold is set too high, it can incorporate noisy or irrelevant data items, which could affect the interpretability and performance of the model. Furthermore, fitting a T.G.M.M becomes computationally expensive for large datasets or high-dimensional

data because of the rise in computational complexity that occurs with both the number of components and the dimensionality of the data [1,2].

Therefore, to have a more precise treatment, the auras inside the image regions are attracted, and using the intensity of the color, a system is designed and developed using the bivariate model for effective identification of the disease pattern to identify the disease in the earlier stage. In this system, features play a vital role, and the recognition of the disease based on aura is subjected to color identification and its intensity. Therefore, these two features, intensity and color, and the Bivariate Gaussian Mixture Model (B.G.M.M) are derived and developed. The updated parameters for B.G.M.M are obtained using the Expectation Maximization (E.M) algorithm, and for the best feature identification, the Grasshopper Optimization Algorithm (G.O.A) is considered.

Even though our ancient Indians have done much research on human Aura, very little work is projected [3]. Hence, we propose methodologies using optimization techniques, statistical methods, and color imaging features to understand the disease in prior stages better. Color features need to be approximately identified to identify the Aura signals effectively. Even though the RGB color spectrum is considered the primary element in interpreting the color of the Aura, the H.S.I color spectrum plays a significant role. Hence, this article considers the H.S.I spectrum and identifies features based on the meta-heuristic algorithm G.O.A. The data sets of Biowell imaging (Aura images) and M.R.I images of the brain are considered to determine the diseases more precisely. The critical point of this model is that it considers two features at once, which aids in improved identification, especially about medical imaging.

Our contribution to this research is:

1. We considered the human Aura image to identify the disease before its appearance in the human body by placing the high-intensity region in the image.
2. We derived B.G.M.M updated model parameter $\mu 1$, $\sigma 1$ and $\mu 2$, $\sigma 2$ mean and variance of feature 1 and feature 2 (i.e., hue and saturation) using E.M algorithm.
3. We have considered the G.O.A algorithm among the various algorithms in our approach. The main advantage is that it searches for the optimal feature by which disease identification can be more appropriate.

The detailed mathematical model of B.G.M.M is presented in methodology section 2 of the article, and also the G.O.A algorithm and data set considered are briefly explained in section 2. The result obtained, and the discussion is presented in section 3 of the article. Section 4 of the article summarizes and concludes with future scope.

2 Methodology

2.1 Bivariate Gaussian Mixture Model

A combination of various Gaussian distributions with varying means and covariances creates the data points in this model. The Expectation-Maximization (E.M) approach is most commonly used to estimate model parameters such as the means and covariances of the various Gaussian components [4]. The E.M. algorithm optimizes these parameters iteratively to fit the observed data best.

PDF of B.G.M.M is given by

$$f(x_1,x_2) = \frac{1}{2\pi\sigma_1\sigma_2(\sqrt{1-p^2})} e^{-\left[\frac{1}{2(1-\rho^2)}\left[\left(\frac{x_1-\mu_1}{\sigma_1}\right)^2 - 2\rho\left(\frac{x_1-\mu_1}{\sigma_1}\right)\left(\frac{x_2-\mu_2}{\sigma_2}\right) + \left(\frac{x_2-\mu_2}{\sigma_2}\right)^2\right]\right]} \tag{2.1}$$

μ_1, μ_2 are any real numbers

$$\sigma 1 > 0,\ \sigma 2 > 0;\ -1 \leq \rho \leq 1 \tag{2.1.1}$$

where $\mu 1$, $\sigma 1$ are the mean and variance of the image with 1st features and $\mu 2$, $\sigma 2$ is the mean and variance of the image with the 2nd features, ρ is called the shape parameter.

If ρ=0 this implies correlation (x, y) = 0.

(i.e.)

$$f(x1,x2) = \frac{1}{2\pi\sigma 1\sigma 2(\sqrt{1-p2})} e^{-\left[\frac{\left[\left(\frac{x_1-\mu_1}{\sigma_1}\right)^2 + \left(\frac{x_2-\mu_2}{\sigma_2}\right)^2\right]}{2}\right]} \tag{2.2}$$

$$= f(x_1)\, f(x_2) \tag{2.3}$$

(i.e.) x and y standard normal variates.

Estimation of model parameters using E.M Algorithm

For efficient image segmentation, it is customary to identify the parameters of the image; for identifying the image regions, the E.M. algorithm proposed by Mc. Lanchan et al. (1997) is used.

Let (x1, xn) (y1, yn) be the features of the training image and assume that each image region is characterized by B.G.M.M given in Equation (2.1.1). The likelihood functions of the image regions. Let (x1, xn) (y1, yn) extracted from image regions of the training image be characterized by using the PDF of the B.G.M.M,

$$h(A,\theta) = \sum_{i=1}^{K} \alpha_i\, g(A_3,\ \theta) \tag{2.4}$$

where $\Theta = (\mu_1\ \sigma_1, \mu_2\ \sigma_2, \rho)$ is given by

$$L(\theta)\ =\ \prod_{i=1}^{N} \left(\sum_{i=1}^{K} \alpha_i g_i(A_3,\ \theta)\right) \tag{2.5}$$

$$= \prod_{i=1}^{N} \left(\sum_{i=1}^{K} \alpha_i \frac{1}{2\pi\sigma_1\sigma_2(\sqrt{1-p^2})} e^{-\left[\frac{1}{2(1-\rho^2)}\left[\left(\frac{x_1-\mu_1}{\sigma_1}\right)^2 - 2\rho\left(\frac{x_1-\mu_1}{\sigma_1}\right)\left(\frac{x_2-\mu_2}{\sigma_2}\right) + \left(\frac{x_2-\mu_2}{\sigma_2}\right)^2\right]\right]} \right) \tag{2.6}$$

$$= log\left(\sum_{i=1}^{K} \alpha_i g_i\ (A_S,\ \theta)\right) \tag{2.7}$$

$$= \sum_{S=1}^{w} log\left(\sum_{i=1}^{K} \alpha_i g_i\ (A_s,\ \theta)\right) \tag{2.8}$$

The primary step of E.M algorithm requires to estimates some resemble initial estimates for the parameters from image region. The idea of E.M algorithm is to compute the maximum likelihood of 'Θ', the unknown parameter.

E- STEP

Here the Log l (Θ) w.r.t. the initial vector is calculated using

$$Q\ (\theta,\ \theta^{(0)}) = E_g\ (s)\ \{logL(\theta)\ |\ A\} \tag{2.9}$$

$$=\ \left(\left(\int_A Log\ \ (L\ (\theta))\,|A)\ h(A_s,\ \theta^{(0)}\right)\right) dz \tag{2.10}$$

$$= \sum_{s=1}^{N} log\,(A_s,\ \theta) \int_Z h\ \left(A,\ \theta^{(0)}\right) dz \tag{2.11}$$

$$= \sum_{s=1}^{N} logg\,(A_s,\ \theta) \tag{2.12}$$

$$= logL\,(\theta) \tag{2.13}$$

$$= \sum_{s=1}^{N} log\left(\sum_{i=1}^{k} \alpha_i g_i\,(A_s,\ \theta)\right) \tag{2.14}$$

The initial estimates of $\Theta^{(i)}$ are computed using

$$h\,(A_s,\ \theta) = \sum_{i=1}^{k} \prod_{i}^{(i)} g_i\left(A_s,\ \theta^{(i)}\right) \tag{2.15}$$

$$= \prod_{i=1}^{N}\left[\sum_{i=1}^{k} \alpha\ \frac{1}{2\pi\sigma_1\sigma_2(\sqrt{1-p^2})} e^{-\left[\frac{1}{2\,(1-\ \rho^2)}\left[\left(\frac{x_1-\mu_1}{\sigma_1}\right)^2 - 2\rho\left(\frac{x_1-\mu_1}{\sigma_1}\right)\left(\frac{x_2-\mu_2}{\sigma_2}\right) + \left(\frac{x_2-\mu_2}{\sigma_2}\right)^2\right]\right]}\right] \tag{2.16}$$

And the conditional probability of any pixel As, drawn from the image region k is given by

$$t_k\ (A_s,\ \theta^{(i)} = \frac{\alpha_k{}^{(i)} g_i(A_s,\ \theta^{(i)})}{h(A_s,\ \theta^{(i)}} \tag{2.17}$$

$$= \frac{\alpha_k{}^{(i)} g_k(A_s,\ \theta^{(i)}}{\sum_{i=1}^{k} \alpha_i{}^{(i)} g_i\left(A_s,\ \theta^{(i)}\right)} \tag{2.18}$$

Since

$$h\left(A_s, \theta^{(i)}\right) = \sum_{i=1}^{k} \alpha_k^{(i)} g_k(A_s,\ \theta^{(i)}) \tag{2.19}$$

Evaluating the expectation

$$Q\left(\theta,\ \theta^{(i)}\right) = E_{\theta^{(i)}}\left\{log\,(L(\theta))\right\} \tag{2.20}$$

Following the heuristics of Blims. J (1997), we have

$$Q\left(\theta,\ \theta^{(i)}\right) = \sum_{i=1}^{k}\sum_{s=1}^{N} E^{(i)}\left\{t_i\ \left(A,\ \theta^{(i)}\right)\left(log\,(g_i\,(A_s,\ \theta) + log\,(\alpha_i))\right)\right\} \tag{2.21}$$

$$and\ g\ \ (A,\ \theta) = \frac{1}{2\pi\sigma_1\sigma_2(\sqrt{1-p^2})} e^{-\left[\frac{1}{2\,(1-\ \rho^2)}\left[\left(\frac{x_1-\mu_1}{\sigma_1}\right)^2 - 2\rho\left(\frac{x_1-\mu_1}{\sigma_1}\right)\left(\frac{x_2-\mu_2}{\sigma_2}\right) + \left(\frac{x_2-\mu_2}{\sigma_2}\right)^2\right]\right]} \tag{2.22}$$

Therefore,

$$Q\ \left(\theta,\ \theta^{(i)}\right) = \sum_{i=1}^{k}\sum_{j=1}^{N} E^{(i)}\left\{t_i\left(A_s,\ \theta^{(i)}\right)\left[log\left(\frac{1}{2\pi X} e^{\frac{-1}{2\left((1-\ e^2\right)}}\right)[R-2BC+Q]\right] + log\alpha_i\right\} \tag{2.23}$$

where

$$X = \left(\frac{x_1 - \mu_1}{\sigma_1}\right)^2 \text{ and } R = BCQB = \left(\frac{x_1 - \mu_1}{\sigma_1}\right), C = \left(\frac{x_2 - \mu_2}{\sigma_2}\right) \text{ and } Q = \left(\frac{x_2 - \mu_2}{\sigma_2}\right)^2 \tag{2.24}$$

M. STEP

For the estimation of model parameters, we need to maximize $Q\left(\theta,\ \theta^{(i)}\right)$ such that

$$\sum_{i=1} \alpha_i = 1 \tag{2.25}$$

This can be solved by equating the log likelihood to zero.

Hence,

$$\frac{\partial}{\partial \alpha_i} = 0 \tag{2.26}$$

$$\frac{\partial}{\partial \alpha_i}\left[\sum_{i=1}^{K}\sum_{s=1}^{N} t\ \left(A_s,\ \theta^i\right) log\left[\frac{1}{2\pi X} e^{\frac{-1}{2(1-\ e^2)}(R - 2\,BC + Q)}\right] + log\left(\alpha_i\right)\right] + \lambda\ \left(1 - \sum_{i=1}^{k} \alpha_i\right) = 0 \tag{2.27}$$

$$\Rightarrow \sum_{i=1}^{N} \frac{1}{\alpha_i} t_i\ \left(A,\ \theta^{(i)}\right) + \lambda = 0 \tag{2.28}$$

Summing both sides, we get λ = - λ

$$\Rightarrow\ \widehat{\alpha_i} = \frac{1}{N}\sum_{i=1}^{N} t_i\left(A_s,\ \theta^i\right) \tag{2.29}$$

Therefore, the updated equation for α – for the (I + 1) estimate is

$$\alpha^{(i+1)} = \frac{1}{N}\sum_{i=1}^{N} t_i\left(A_s,\ \theta^{(i)}\right) \tag{2.30}$$

In order to Update μ_1, one has to consider the derivative of $Q\ \left(\theta,\ \theta^{(i)}\right)$ with respect to μ_1= 0 and equate it to zero.

$$i.e.\ \ \frac{\partial Q}{\partial \mu_1}\left(\theta,\ \theta^{(i)}\right) = 0 \tag{2.31}$$

$$= \frac{\partial Q}{\partial \mu_1} = \frac{1}{2\pi\ \sigma_1\sigma_2} e^{-\left[\frac{1}{2(1-\ \rho^2)}\left[\left(\frac{x_1 - \mu_1}{\sigma_1}\right)^2 - 2\rho\left(\frac{x_1 - \mu_1}{\sigma_1}\right)\left(\frac{x_2 - \mu_2}{\sigma_2}\right) + \left(\frac{x_2 - \mu_2}{\sigma_2}\right)^2\right]\right]} - \left[\frac{1}{2\pi\sigma_1\sigma_2(\sqrt{1-p^2})} e^{-\left[\frac{1}{2(1-\ \rho^2)}\left[\left(\frac{x_1 - \mu_1}{\sigma_1}\right)^2 - 2\rho\left(\frac{x_1 - \mu_1}{\sigma_1}\right)\left(\frac{x_2 - \mu_2}{\sigma_2}\right) + \left(\frac{x_2 - \mu_2}{\sigma_2}\right)^2\right]\right]}\right] \tag{2.32}$$

$$= \frac{1}{2\ (1-\ p^2)}\left\{2\left(\frac{x_1 - \mu_1}{\sigma_1}\right)\left(\frac{-1}{\sigma_1}\right) + \frac{2p}{\sigma_1}\left(\frac{x_2 - \mu_2}{\sigma_2}\right)\right\} = 0 \tag{2.33}$$

Therefore, the updated equation for the mean of the first feature is

$$\mu_1{}^{(i+1)} = e\left(\frac{x_2 - \mu_2}{\sigma_2}\right) = \left(\frac{x_1 - \mu_1}{\sigma_1}\right) \tag{2.34}$$

In order to update the parameter μ_2, the mean of the second feature, we differentiate $Q\left(\theta,\ \theta^{(i)}\right)$ with respect to μ_2 and equate it to zero.

$$i.e.\ \ \frac{\partial Q}{\partial \mu_2} = 0 \tag{2.35}$$

$$= -2\rho\left(\frac{x_1-\mu_1}{\sigma_1}\right)\left(\frac{-1}{\sigma_2}\right)+2\left(\frac{x_2-\mu_2}{\sigma_2}\right)\left(\frac{-1}{\sigma_2}\right)=0 \tag{2.36}$$

The updated parameter for the second feature is

$$\mu_2^{(i+1)} \Rightarrow \frac{2}{\sigma_2}\left[e\left(\frac{x_1-\mu_1}{\sigma_1}\right)-\left(\frac{x_2-\mu_2}{\sigma_2}\right)\right]=0 \tag{2.37}$$

To update the variance of the first feature, we have to find the derivative of $Q\left(\theta,\ \theta^{(i)}\right)$ and differentiate it with respect to σ_1 and equate it to zero.

$$\frac{\partial Q}{\partial \sigma_1} = \frac{1}{2\pi\sigma_2\sqrt{1-\rho^2}}\frac{-1}{\sigma_1^2}e^{\alpha}+\frac{1}{2\pi\sigma_1\sigma_2\sqrt{1-e^2}}\left\{\frac{-e^{\alpha}}{2(1-\rho^2)}\right\}\left[(x_1-\mu_1)^2(-2)\left(\sigma_1^{-3}\right)+2e\left(\frac{x_1-\mu_1}{\sigma_1}\right)\left(\frac{x_2-\mu_2}{\sigma_2}\right)\right] \tag{2.38}$$

$$\Rightarrow \frac{1}{2\pi\sigma_1\sigma_2\sqrt{1-e^2}} = \frac{-1}{2(1-\rho^2)2\pi\sigma_1\sigma_2\sqrt{1-e^2}}\left[(x_1-\mu_1)^2(-2)\left(\sigma_1^{-3}\right)+2\left(\left(\frac{x_1-\mu_1}{\sigma_1}\right)\left(\frac{x_2-\mu_2}{\sigma_2}\right)\right)\right] \tag{2.39}$$

$$\Rightarrow \frac{1}{\sigma_1} = \left[\left[\frac{-2\ (x_1-\mu_1)^2}{\sigma_1^3}\right]+\frac{2e\ (x_1-\mu_1)(x_2-\mu_2)}{\sigma_1^2\sigma_2}\right]-\left(\frac{-1}{2(1-\rho^2)}\right) \tag{2.40}$$

$$\Rightarrow \sigma_1^2 = \left\{-2\ (x_1-\mu_1)^2+\frac{2e\ (x_1-\mu_1)(x_2-\mu_2)}{\sigma_2}\sigma_1\right\}\left\{\frac{-1}{2(1-\rho^2)}\right\} \tag{2.41}$$

$$\Rightarrow {\sigma_1}^2-K_1\sigma_1+K_2=0 \tag{2.42}$$

$$where\ K_1 = \left(\frac{2e(x_1-\mu_1)(x_2-\mu_2)}{\sigma_2}\right)\left(\frac{-1}{2(1-\rho^2)}\right) \tag{2.43}$$

and $K_{2=}\frac{2(x_1-\mu_1)^2}{(1-\rho^2)}$

$$\therefore \sigma_1 = \frac{K_1 \pm \sqrt{{K_1}^2-4K_2}}{2} \tag{2.44}$$

In order to find the updated equation of the second parameter σ_2, we differentiate $Q\left(\theta,\theta^{(i)}\right)$ with respect to σ_2 and equate it to zero.

$$\frac{\partial Q}{\partial \sigma_2} = -\frac{1}{2\pi\sigma_2\sqrt{1-e^2}}e^{\alpha}+\frac{1}{2\pi\sigma_1\sigma_2\sqrt{1-e^2}}e^{\alpha}\left(\frac{-1}{2(1-\rho^2)}\right)\left[+2e\left(\frac{x_1-\mu_1}{\sigma_1}\right)\left(\frac{x_2-\mu_2}{\sigma_2^2}\right)-2\frac{(x_2-\mu_2)^2}{\sigma_2^3}\right]=0 \tag{2.45}$$

$$\Rightarrow \frac{1}{2\pi\sigma_1\sigma_2\sqrt{1-e^2}}e^{\alpha} = \frac{1}{2\pi\sigma_1\sigma_2\sqrt{1-e^2}}e^{\alpha}\left(\frac{-1}{2(1-\rho^2)}\right)\left[\frac{2e\ (x_1-\mu_1)(x_2-\mu_2)}{\sigma_1\sigma_2^2}-2\frac{(x_2-\mu_2)^2}{\sigma_2^3}\right] \tag{2.46}$$

$$\Rightarrow \frac{1}{\sigma_2} = \left(\frac{-1}{2(1-\rho^2)}\right)\left[\frac{2e\ (x_1-\mu_1)(x_2-\mu_2)}{\sigma_1\sigma_2^2}\ 2\frac{(x_2-\mu_2)^2}{\sigma_2^3}\right] \tag{2.47}$$

$$\Rightarrow \sigma_2^2 = \left(\frac{-1}{2(1-\rho^2)}\right)\left[\frac{2e\ (x_1-\mu_1)(x_2-\mu_2)}{\sigma_1}\sigma_2 - 2(x_2-\mu_2)^2\right] \tag{2.48}$$

$$\sigma_2{}^2 + K_3\sigma_2 + K_4 = 0 \tag{2.49}$$

$$where\ K_3 = \frac{1}{2(1-\rho^2)}\frac{2e\ (x_1-\mu_1)(x_2-\mu_2)}{\sigma_1} \tag{2.50}$$

$$and\ K_4 = \frac{-(x_2-\mu_2)^2}{(1-\rho^2)} \tag{2.51}$$

Therefore, the updated equation for the second feature σ_2, is,

$$\therefore\ \sigma_2 = \frac{-K_3 \pm \sqrt{K_3{}^2 - 4K_4}}{2} \tag{2.52}$$

2.2 Grasshopper Optimization Algorithm (G.O.A)

The G.O.A algorithm is nature inspired algorithm. The grasshopper's life cycle is divided into two stages: nymph and adult. It moves slowly with little steps during the nymph phase and quickly and can fly large distances as an adult. The grasshopper's movement was used to mathematically simulate the algorithm. [5]

2.2.1 Grasshopper Optimization Algorithm

- Step 1: Initialize the grasshopper population size and position of each grasshopper.
- Step 2: Find the fitness value for each grasshopper.
- Step 3: Find the initial best position and best fitness value of each grasshopper.
- Step 4: Normalize the distance between the grasshoppers and update the position of each grass hopper.
- Step 5: Check the boundary value for each grasshopper. If it crosses the boundary bring back to its previous position.
- Step 6: Compute the new fitness value for each grasshopper.
- Step 7: If the new fitness value is better than the previous fitness then replaces the current fitness value with old fitness value as best fitness.
- Step 8: Repeat the step 4-7 until stopping criteria is met.
- Step 9: Return the best fitness value and position of the grasshopper.

If the optimal solution is achieved then iteration is stopped else steps 1 to 9 are repeated until the criteria are met. Finally, the G.O.A provides maximal clustering efficiency and accuracy. Each element of G.O.A contains several elements as a count of pixels. Each particle is mapped to a pixel and the pixel value indicates the cluster to which it belongs.

2.3 UCI and Bio-well Dataset

The UCI data collection serves as a central repository for machine learning, including contributions from many people and organizations throughout the world. This repository is used by researchers to study various machine learning algorithms, such as databases, domain theories, and data generators. The data collection covers a wide range of applications, from physics to biology, and includes information such as the number of characteristics, attribute types, instances, and publication years to facilitate sorting and searching. Human biofield images were acquired utilizing specialized devices known as gas discharge visualization (GDV) or electro photonic imaging (EPI) technology, which was developed by a group of scientists. These data sets are used to analyze disease predictions based on energy levels in biofield pictures. More than 200 scientific publications on EPI/GDV technology have been published in various journals throughout the world, spanning a wide range of topics, including allopathic and integrative medicine, psychology, consciousness studies, sports, and fundamental research.

3 Results and Discussion

In this article, the G.O.A based optimization technique is considered for the identification of the features of the disease/damaged tissues to find the deformities in the medical images. These features are given as input to the G.M.M-E.M algorithm. The G.M.M-E.M algorithm is divided into two phases: initialization and finalization. Initial estimates are derived using the K-Mean technique, and final estimates are obtained using the Mc. Lanchan heuristic. K-Mean clustering helps to identify the features. These features need to be effective to improve the accuracy and efficiency of the clustering. The k-Mean algorithm has a drawback in terms of sensitivity. Optimization techniques will be more effective in overcoming this issue. In this article, G.O.A. is considered for this purpose because of its properties, such as removing redundant data and being effective in feature selection. The features derived from optimization strategies are fed into the final parameters and segmentation process. Separate experiments were carried out for M.R.I. pictures and aura images. The efficiency of the results obtained for MRI-based images is compared to existing algorithms based on clustering and classification techniques using image quality metrics such as average distance, image noise, peak signal-to-noise ratio, mean square error (M.S.E.), and ISNR[6,7]. The experimentation was also conducted by employing an aura image. Figure 1 shows the diseased aura image considered for the experimentation. The image on the left shows health issues in the throat chakra, solar plexus, and root chakra. The image on the right shows the segmented image, and Figure 2 shows the brain image with sub-regions.

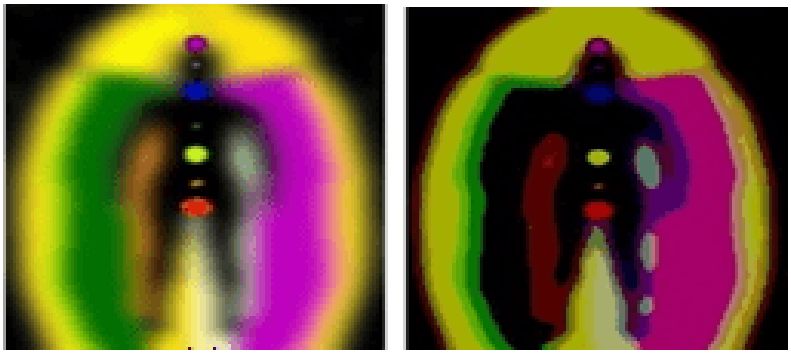

Fig 1. Input aura image and the segmented image

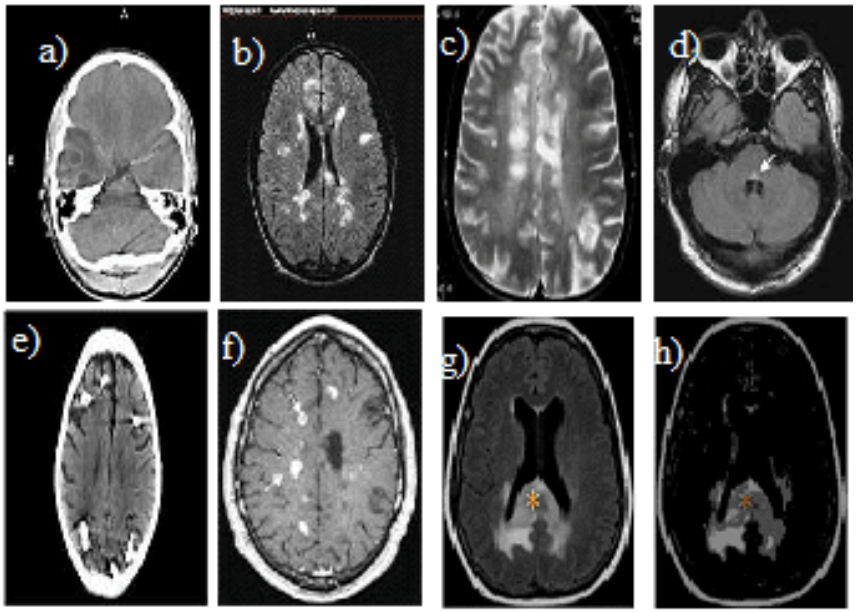

Fig 2. Brain image with CSF, WM and Grey Matter (a-h)

We tested our algorithm on two images, C0 and C1, which contain four subregions: brain image with CSF (C0SB1 and C1SB1), brain image with W.M. (C0SB2 and C1SB2), brain image with Grey Matter (C0SB3 and C1SB3), and brain image with background (C0SB4 and C1SB4). Each pixel in the image region is assumed to have a Gaussian distribution, and the overall image is assumed to be a combination of these Gaussian distributions. After obtaining revised estimates, the picture reconstruction is subjected to the E.M. algorithm. Objective assessment techniques such as the Jaccard Coefficient (J.C.), Volume of Similarity (V.S.), and others are used to evaluate segmentation models [8,9]. The result obtained using quality metrics for both the proposed model B.G.M.M and the existing G.M.M with the E.M. model is tabulated in Table 1.

Table 1. Segmentation Metrics used for detection of Seizures

Image	Quality Metrics	G.M.M with E.M	Bivariate G.M.M with KM
C0SB1	Jaccard coefficient	0.089	0.795
	Volume Similarity	0.432	0.891
	Variation of information	2.3665	5.232
	Global consistency error	0.2180	0.4223
	Probabilistic random index	2 0.504	0.7958
C0SB2	Jaccard Coefficient	0.0677	0.819
	Volume of Similarity	0.3212	0.8914
	Variation of information	1.9724	6.2894
	Global consistency error	0.2144	0.4664
	Probabilistic random index	3 0.416	0.6847
C0SB3	Jaccard Coefficient	0.0434	0.784
	Volume of Similarity	0.123	0.926
	Variation of information	0.7684	5.5318
	Global consistency error	0.089	0.4001
	Probabilistic random index	0.576	0.706
C0SB4	Jaccard Coefficient	0.0456	0.911
	Volume of Similarity	0.2123	0.643
	Variation of information	3 1.268	4.1619
	Global consistency error	0.056	0.21949
	Probabilistic random index	0.189	0.5628
C1SB1	Jaccard Coefficient	0.141	0.826
	Volume of Similarity	0.313	0.7910
	Variation of information	1.6499	4.4115
	Global consistency error	0.1874	0.21752
	Probabilistic random index	0.9256	0.686
C1SB2	Jaccard Coefficient	0.098	0.896
	Volume of Similarity	0.0433	0.918
	Variation of information	2.3215	6.6411
	Global consistency error	0.21838	0.4661
	Probabilistic random index	0.3807	0.6322
C1SB3	Jaccard Coefficient	0.0222	0.946
	Volume of Similarity	0.3223	0.3869
	Variation of information	1.2411	6.7129
	Global consistency error	0.1466	0.4559
	Probabilistic random index	0.9576	0.7202
C1SB4	Jaccard Coefficient	0.455	0.854
	Volume of Similarity	0.329	0.786
	Variation of information	1.816	5.0898
	Global consistency error	0.119	0.3062
	Probabilistic random index	0.065	0.5573

The recovered medical image's performance is achieved using subjective and objective quality testing. The objective quality testing methodologies are most frequently used and compared to the segmentation evaluation technique. Since the objective methodologies are performed with respect to numerical formulas, it allows the comparison of different algorithms.

The segmentation outputs obtained are evaluated using segmentation QM, which includes JC, VS, VOI, GCE, and PRI. Table 2 shows the result obtained for aura images. From Tables 1 and 2, it is observed that the value obtained for the quality metrics nearer to 0 indicates that the proposed model performs well in identifying the deformity in both medical images as well as aura images.

Table 2. Result comparison with proposed method B.G.M.M with G.M.M

Image	Quality Metrics	Gaussian Mixture Model with E.M	Bivariate G.M.M with KM
C0SB1	Jaccard Coefficient	0.079	0.612
	Volume Similarity	0331	0.654
	Variation of information	2.453	5.116
	Global consistency error	0.234	0.587
	Probabilistic random index	0.654	0.789
C0SB2	Jaccard Coefficient	0.0655	0.843
	Volume Similarity	0.342	0.8654
	Variation of information	1.654	6.345
	Global consistency error	0.233	0.4675
	Probabilistic random index	0.456	0.6765
C0SB3	Jaccard Coefficient	0.04467	0.784
	Volume Similarity	0.1678	0.926
	Variation of information	0.7684	5.5318
	Global consistency error	0.0834	0.4001
	Probabilistic random index	0.678	0.706
C0SB4	Jaccard Coefficient	0.04345	0.911
	Volume Similarity	0.2435	0.643
	Variation of information	1.453	4.1619
	Global consistency error	0.123	02322
	Probabilistic random index	0.189	0.53458

4 Conclusion

The article highlights the methodology based on the G.O.A experimentation technique together with a model-based approach using the G.M.M algorithm for effective identification of disease inside the medical images, and the work is extended to identify the deformity in aura images. The outcomes are tabulated and computed using existing methods as well as quality metrics. The testing is performed on the benchmark data set. The results showcase that the performance of the developed methods identifies the various damaged tissues inside the medical images acquired through MRI and also identifies the high-intensity energy regions where a possible deformity is associated with the aura images. With the help of the proposed algorithm, it is possible to visualize the edges more effectively, and the results presented in the above table justify the same. Since the edges are more visible, it helps to have a broad range of images, and this helps in a better understanding of the medical images. The presented proposed methodology facilitates the investigation of the images in a better discrepancy than that of the current models.

References

1) Poojary M, Srinivas Y. Optimization Technique Based Approach for Image Segmentation. *Current Medical Imaging Reviews*. 2023;19(10):1167–1177. Available from: https://dx.doi.org/10.2174/1573405619666221104161441.
2) Poojary M, Srinivas Y. A Novel Methodology for Disease Identification Using Metaheuristic Algorithm and Aura Image. *International Journal of Advanced Computer Science and Applications*. 2022;13(7):590–594. Available from: https://dx.doi.org/10.14569/ijacsa.2022.0130770.
3) Chhabra G, Prasad A, Marriboyina V. Implementation of aura colourspace visualizer to detect human biofield using image processing technique. *Journal of engineering science and technology*. 2019;14(2):892–908. Available from: https://www.researchgate.net/publication/335419618_IMPLEMENTATION_OF_AURA_COLOURSPACE_VISUALIZER_TO_DETECT_HUMAN_BIOFIELD_USING_IMAGE_PROCESSING_TECHNIQUE.
4) Riaz F, Rehman S, Ajmal M, Hafiz R, Hassan A, Aljohani NR, et al. Gaussian Mixture Model Based Probabilistic Modeling of Images for Medical Image Segmentation. *IEEE Access*. 2020;8:16846–16856. Available from: https://dx.doi.org/10.1109/access.2020.2967676.
5) Meraihi Y, Gabis AB, Mirjalili S, Ramdane-Cherif A. Grasshopper Optimization Algorithm: Theory, Variants, and Applications. *IEEE Access*. 2021;9:50001–50024. Available from: https://dx.doi.org/10.1109/access.2021.3067597.
6) Hamada MA, Kanat Y, Abiche AE. Multi-Spectral Image Segmentation Based on the K-means Clustering. *International Journal of Innovative Technology and Exploring Engineering*. 2019;9(2):1016–1019. Available from: https://dx.doi.org/10.35940/ijitee.k1596.129219.

7) Rosyadi AW, Suciati N. Image segmentation using transition region and k-means clustering. *International Journal of Computer Science*. 2020;47(1):47–55. Available from: https://www.iaeng.org/IJCS/issues_v47/issue_1/IJCS_47_1_06.pdf.
8) Karanam SR, Srinivas Y, Chakravarty S. A systematic approach to diagnosis and categorization of bone fractures in X-Ray imagery. *International Journal of Healthcare Management*. 2022;p. 1–12. Available from: https://dx.doi.org/10.1080/20479700.2022.2097765.
9) Sivanarayana GV, Kumar KN, Srinivas Y, Kumar GVSR. Review on the Methodologies for Image Segmentation Based on CNN. In: Communication Software and Networks;vol. 134 of Lecture Notes in Networks and Systems. Singapore. Springer. 2021;p. 165–175. Available from: https://doi.org/10.1007/978-981-15-5397-4_18.